

Supplementary Information for

Adipose tissue NAD⁺ biosynthesis is required for regulating adaptive thermogenesis and whole-body energy homeostasis in mice

Shintaro Yamaguchi^{1*}, Michael P. Franczyk^{1*}, Maria Chondronikola¹, Nathan Qi², Subhadra C. Gunawardana³, Kelly L. Stromsdorfer¹, Lane C. Porter¹, David F. Wozniak⁴, Yo Sasaki⁵, Nicholas Rensing⁶, Michael Wong⁶, David W. Piston³, Samuel Klein^{1,3}, Jun Yoshino^{1,7}

¹Center for Human Nutrition, ³Department of Cell Biology and Physiology, ⁴Department of Psychiatry and the Taylor Family Institute for Innovative Psychiatric Research, ⁵Department of Genetics, ⁶Department of Neurology, and ⁷Department of Developmental Biology, Washington University School of Medicine, St. Louis, MO 63110.

²Department of Molecular and Integrative Physiology, University of Michigan, Ann Arbor, MI 48109.

*These authors equally contributed to this study.

Corresponding author:

Jun Yoshino, M.D., Ph.D.

E-mail: jyoshino@wustl.edu

This PDF file includes:

Materials and Methods

Figs. S1 to S9

Tables S1 to S2

References for SI reference citations

SI Materials and Methods

Animal experimentation

ANKO mice were generated by using *Adiponectin*-Cre transgenic mice and floxed-*Nampt* (flox/flox) mice (1) as described previously (2, 3). BANKO mice were generated by using *Ucp1*-Cre transgenic mice and flox/flox mice. Mice were housed at normal room temperature (22 °C) or thermoneutrality (30 °C) with 12-h light/12-h dark cycles and were maintained on a regular chow diet (LabDiet) *ad libitum*. For cold exposure experiments, mice were kept at 4 °C and rectal temperature, BAT temperature, VO₂, and EMG were measured. For NMN rescue experiments, we administered NMN in drinking water at the approximate dose of 500 to 1000 mg/kg of body weight, to mice for up to 8 weeks (3). NMN was purchased from Botanc Bio-engineering and Oriental Yeast Co. Ltd.

Human studies

Thirteen women with overweight or obesity (age 36.6 ± 2.6 years, BMI 31.0 ± 0.7 kg/m²) participated in this study (Table S1) (Clinical Trials.gov NCT02786251). All participants completed a comprehensive screening evaluation that included a medical history and physical examination, standard blood tests, and an oral glucose tolerance test. Potential participants were excluded if they had diabetes or other serious diseases, smoked cigarettes, consumed excessive alcohol (men who consume >21 units of alcohol per week and women who consume >14 units of alcohol per week), were pregnant or lactating, received radiation exposure for research purposes during the last year, or had metal implants that interfered with the imaging procedures.

Each participant completed one cold exposure (CE) and one thermoneutral (TN) study visit, two to four weeks apart in a randomized, cross-over fashion. Participants were asked to maintain their usual diet and refrain from excessive physical activity and consumption of alcohol, spices, and caffeine for at 3 days before each study visit. For the CE study visit, participants were admitted to the Clinical and Translational Research Unit (CTRU) the night before the study. At 0700 h, after participants fasted for ~10 h overnight, a 6 hour standard cooling protocol was performed to maximize non-shivering thermogenesis (4, 5). Participants wore shorts, a hospital gown, and a liquid conditioned wrap (ThermoWrap, Belmont Medical Technologies, Billerica, MA) while resting in bed. The liquid conditioned wrap temperature was initially set at ~22°C and was decreased by 1°C

intervals every ~60 minutes until shivering occurred. Immediately upon shivering, cooling equipment temperature was increased by ~1-2°C until shivering subsided. For the TN study visit, participants were admitted to the CTRU at ~0700 h after fasting for ~10 h at home. Participants rested in bed at a room temperature of ~26-28°C while wearing shorts and hospital gown. After 6 hours of CE or TN conditions, participants were transferred by wheelchair to the Center for Clinical Imaging Research, which is a few minutes from the CTRU, where adipose tissue samples were obtained by an experienced interventional radiologist. A positron emission tomography and computed tomography-guided percutaneous needle biopsy technique was used to obtain samples from the supraclavicular area (6), where BAT is localized in people (7-9).

Indirect calorimetry

The rate of whole-body oxygen consumption (VO_2) was determined by using a Phenomaster system (TSE Systems, Bad Homburg, Germany), an Oxymax indirect calorimetry system (Columbus Instruments, Columbus, OH), or a Comprehensive Lab Animal Monitoring System (CLAMS, Columbus Instruments). Data expressed per mouse were analyzed and presented. All experiments were conducted at the Washington University Diabetes Models Phenotyping Core of the Diabetes Research Center (DRC) and University of Michigan Mouse Metabolic Phenotyping Center (MMPC).

Cold tolerance test

Mice were kept on aspen bedding at 4 °C in a cold room and rectal core body temperature was monitored using a rectal probe in individually-caged mice. We also evaluated the effects of cold exposure on BAT temperature by using the implanted chips (see the details below). In this study, mice were semi-fasted overnight with 0.5 g of food and BAT temperature was monitored before and after cold exposure.

BAT temperature monitoring

To monitor BAT temperature, mice underwent the surgery procedure to have the IPTT-300 temperature chips (Bio Medic Data Systems) implanted subcutaneously in direct contact to the BAT. BAT temperature

recordings were taken manually using a temperature scanner (DAS-7007; Bio Medic Data Systems) before and after cold exposure and norepinephrine injection at the University of Michigan MMPC.

Electromyography (EMG) studies

Custom wire EMG electrode sets were constructed using six Teflon coated stainless steel wires (76 um bare diameter) soldered to an electronic pin header with approximately 2mm of exposed tip. The soldered contacts were covered with dental cement and a stainless steel micro screw was soldered to the end of two wires to provide an electrical ground and an anchor to the skull. The electrode set was sterilized for implantation and mice were placed under 2% isoflurane on a stereotaxic frame with a heating pad set to 36.5°C until pedal withdraw reflex ceased. Two bilateral EMG recording wires were placed under the nuchal muscles with the exposed tip secured into the muscle. The exposed skull, screws, and wires were secured and covered in a layer of dental cement (SNAP, Parkell) with the pin header secured to the head for subsequent recording.

Mice recovered from surgery for 48 hours and were connected to recording amplifiers with a flexible custom cable attached to the exposed electronic pins on the head. Mice were acclimated and tethered for at least 1-hour prior to being transferred to a 4°C cold room to record EMG activity for one hour. Bilateral nuchal EMG signals were acquired using a differential montage by single channel amplifiers (P511, Grass). Signals were amplified at 10,000X with high-pass (10Hz) and low-pass (300Hz) filters applied. EMG signals were digitized and recorded at 500Hz using a DAQ (MP150, BioPac) and time-locked video acquisition software (AcqKnowledge 4.4, BioPac). Digital EMG signals (.edf) were imported into LabChart 8.1 software and converted to root mean square (RMS) activity using 100ms windows with triangular (Bartlett) averaging. After excluding movement artifact, RMS activity was analyzed for shivering bursts using 10 second epochs and epochs were averaged across the cold exposure period.

Body composition and glucose and lipid metabolism

Body composition was determined using a NMR instrument (EchoMRI, Echo Medical Systems LLC, Waco, TX). For intraperitoneal glucose tolerance tests (IPGTTs), 50 % dextrose solution (2 g/kg-total body weight) was injected after mice were fasted for approximately 15 hours. For insulin tolerance tests (ITTs), mice

were injected with human insulin (0.75 U/kg-total body weight) after they were fasted for approximately 4 hours. Tail blood was taken during the IPGTTs and ITTs, and glucose levels were measured by using the Accu-Chek II glucometer (Roche Diagnostics, Indianapolis, IN) as previously described (3, 10). Plasma concentrations of triglyceride (TG), total cholesterol, and free fatty acids (FFA), and hepatic TG contents were determined at the DRC Animal Model Research Core as described previously (3, 10). Plasma insulin concentrations were determined by using the Erenna immunoassay system (Singulex, Alameda, CA). Plasma adiponectin concentrations were measured by using ELISA kits that were developed and provided by Oriental Yeast Co. Ltd.

Locomotor activity

Locomotor activity was assessed over a 1-hour period using transparent polystyrene enclosures (47.6 x 25.4 x 20.6 cm) and computerized photobeam instrumentation in the Washington University Animal Behavioral Core (ABC) as described previously (3). Total ambulations (whole body movements) were quantified and summed for each of 6, 10-min blocks.

Norepinephrine injection experiment

Mice were individually placed into the sealed chambers (7.9" x 4" x 5") in the CLAMS and acclimated under the thermoneutral conditions (30°C). To inhibit physical activity, mice were anesthetized with an intraperitoneal injection of 70-80 mg/kg pentobarbital. Norepinephrine (L-(-)-Norepinephrine (+)-bitartrate salt monohydrate; Sigma Aldrich) or vehicle (PBS) was then injected subcutaneously at a 1 mg/kg dose and VO₂ values and BAT temperature were monitored before and after norepinephrine or PBS injection as described above.

CL-316243 injection experiment

We determined the effect of systemic β 3-adrenergic stimulation on VO₂ by using an Oxymax indirect calorimetry system (Columbus Instruments). Mice were injected intraperitoneally with CL-316243 (#C5976; Sigma, St. Louis, MO) (0.6 mg/kg-body weight) at 9-11 AM after overnight acclimation period.

NAD⁺ metabolomics

LC/MS/MS: For NAD⁺ metabolites measurements, BAT samples were homogenized in 50 % methanol/water and chloroform. The samples were loaded onto an Agilent 1290 HPLC system equipped with an Atlantis T3 column (Waters) as described previously (10, 11). Data were normalized by tissue weight.

HPLC: NAD⁺ was extracted from frozen mouse tissue samples and OP9 adipocytes by using ice-cold perchloric acid. NAD⁺ concentrations were determined using an HPLC system (Prominence; Shimadzu Scientific Instruments, Columbia, MD) with a Supelco LC-18-T column (#58970-U; Sigma) as described previously (3, 12). NAD⁺ concentrations were normalized to tissue weights or amount of protein.

RNA sequencing (RNA-seq)

Library preparation was performed with 1 µg of total RNA after integrity was determined using an Agilent bioanalyzer (Agilent Technologies). Ribosomal RNA was removed by a hybridization method using Ribo-ZERO kits (Illumina, San Diego, CA). mRNA was reverse transcribed to yield cDNA using SuperScript III RT enzyme (Life Technologies, Gaithersburg, MD) and random hexamers. cDNA fragments were sequenced on an Illumina HiSeq-3000. The fragments per kilobase million reads (FPKM) values were calculated and used for further analyses. Differentially expressed genes (DEGs) (false discovery rate [FDR] < 0.01 and fold change > 2) were determined by using the edgeR R Bioconductor package. Functional enrichment analyses were performed on DEGs using the Database for Annotation, Visualization, and Integrated Discovery (DAVID) Bioinformatics Resources 6.8 (<http://david.abcc.ncifcrf.gov/>) with Gene ontology biological process (GO BP) Direct category. GO terms with a FDR < 0.05 were considered to be significantly enriched and redundant GO terms were removed by REVIGO program (<http://revigo.irb.hr/>). All RNA-seq data used in this study have been deposited into the NCBI GEO database under accession number GSE137149.

Real-time PCR

The relative expression was determined by normalizing the Ct value to the housekeeping control gene, ribosomal protein (*36b4* for mouse, *RPLP0* for human genes). Data were log-transformed for statistical analyses. Primers are listed in Table S2.

Mitochondrial DNA content

DNA was isolated by using QIAamp DNA Mini Kit (#51034, Qiagen). Mitochondrial DNA (mtDNA) contents were determined by quantitating expression of 16S ribosomal RNA (rRNA) (forward: 5'-CCGCAAGGGAAAGATGAAAGAC-3'; reverse: 5'-TCGTTTGGTTTCGGGGTTTC-3') and a nuclear-encoded gene, hexokinase 2 (forward: 5'-GCCAGCCTCTCCTGATTTTAGTGT-3'; reverse: 5'-GGGAACACAAAAGACCTCTTCTGG-3') as described previously (10).

Mitochondrial activity

Mitochondria were isolated from BAT using sucrose step density gradient as we previously described (10). The enzyme activities of the ETC complex-I and -IV were evaluated using the commercially available microplate assay kits (Abcam, #ab109721 and #109911 respectively) following the manufacture's instruction. ATP contents were determined in BAT mitochondria by using the LC/MS/MS system as described above.

Western blot

Extracted protein samples were loaded onto polyacrylamide gels, separated by SDS-PAGE, and transferred to PVDF membranes. The blotted membranes were incubated with the following primary antibodies: rabbit monoclonal anti-NAMPT antibody (#86634, Cell Signaling Technology, Beverly, MA), mouse monoclonal anti- α -TUBULIN (#T5168, Sigma), total OXPHOS antibody cocktail (#ab110413; Abcam, Cambridge, UK), rabbit polyclonal anti-Transferrin antibody (ab82411, Abcam), rabbit monoclonal anti-Caveolin-1 (CAV1) antibody (#3267, Cell Signaling Technology), rabbit monoclonal anti-Insulin receptor β (IR β) antibody (#3025, Cell Signaling Technology), mouse monoclonal anti-phospho-Perilipin-1 (Ser522) antibody (#4856, Vala Sciences, San Diego), rabbit monoclonal anti-Perilipin-1 antibody (#9349, Cell Signaling Technology), rabbit polyclonal anti-phospho-HSL (Ser563) antibody (#4139, Cell Signaling Technology), and

rabbit polyclonal anti-HSL antibody (#4107, Cell Signaling Technology). All blots were incubated with horseradish peroxidase (HRP)-linked anti-rabbit antibody (#7074, Cell Signaling Technology) or HRP-linked anti-mouse antibody (#sc-2005, Santa Cruz Biotechnology), and developed by using the ECL Western Blotting Detection Reagent. Western blot densitometry was quantitated using ImageJ software (NIH ImageJ 1.47; <http://imagej.nih.gov/ij>).

Lipolysis assays

In vivo: CL-316243 (1 mg/kg-body weight) was intraperitoneally injected into mice. Blood was collected before and 15- and 30-min after CL-316243 injection. Blood and plasma samples were used for measurements of glucose, glycerol (Sigma), and FFA (Wako Chemicals).

Ex vivo: The visceral WAT were surgically removed from mice. WAT tissue pieces were incubated in phenol red-free DMEM containing 2% fatty acids-free BSA in the presence or absence of 1 μ M isoproterenol (Sigma) for 2 hours at 37 °C. The culture medium was collected for glycerol measurements. Data were normalized by tissue weight.

In vitro: Glycerol release into the medium was also evaluated in OP9 adipocyte cells. OP9 cells were incubated in phenol red-free DMEM containing 2% fatty acids-free BSA in the presence or absence of 1 μ M isoproterenol for 2 hours at 37 °C. The culture medium was collected for glycerol measurements. Data were normalized by protein concentrations.

Cell Culture

The OP9 preadipocytes were maintained in α -MEM supplemented with 20% FBS (propagation medium). To induce adipogenesis, preadipocytes were cultured for 24-48hrs in α -MEM with 0.2% FBS, 175 nM insulin and 900 μ M oleate (3). Differentiated adipocytes were incubated in the propagation medium in the presence or absence of DMSO (control), 750 nM FK866 (Cayman Chemical), 500 μ M NMN (Sigma), and 10 μ M Ex527 (Tocris) for up to 5 days. Differentiated adipocytes were incubated with 100 μ M Accell siRNAs targeting GFP (control) or mouse *Cav1* according to the manufacturer's instruction (Dharmacon).

Statistical analysis

Differences between two groups were assessed by using Student's paired or unpaired t-tests. Differences in continuous metabolic parameters and locomotor activity (total ambulations) were evaluated by using repeated-measures ANOVAs. Comparisons among multiple groups were performed using one-way ANOVA with the Tukey's post hoc test. Data are presented as means \pm SEM. A *P* value less than 0.05 was considered statistically significant.

Supplemental Figure 1

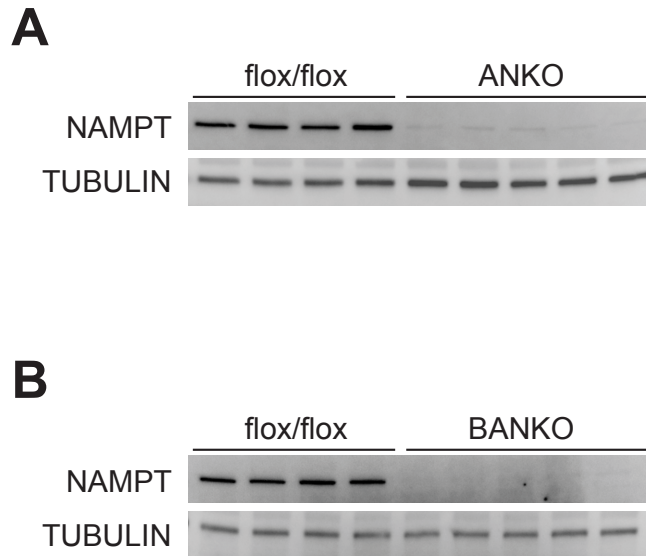


Figure S1. Western blot analysis of NAMPT in BAT.

The protein expression levels of NAMPT and TUBULIN were determined in brown adipose tissue (BAT) obtained from adipocyte-specific *Nampt* knockout (ANKO) (A), brown adipocyte-specific *Nampt* knockout BANKO (B), and their control (flox/flox) mice (n=4-5 per group).

Supplemental Figure 2

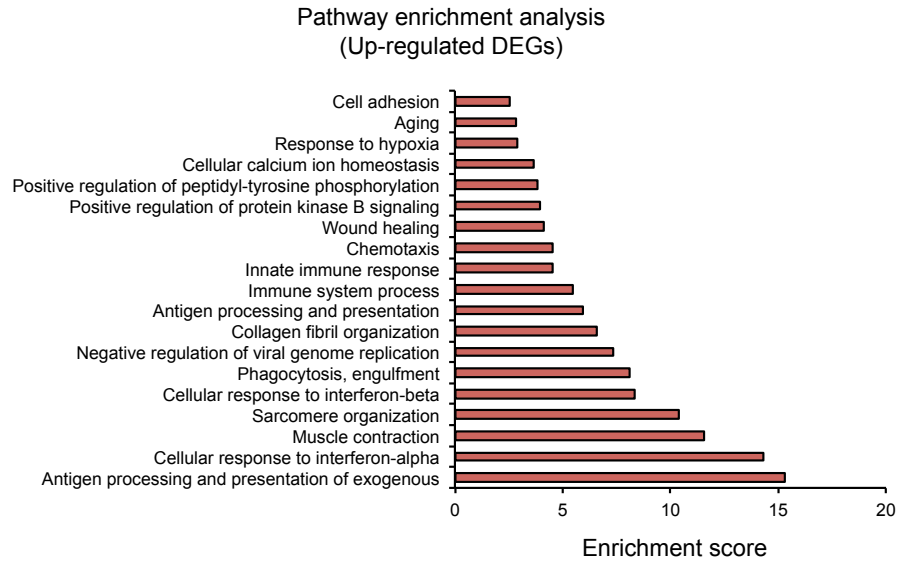


Figure S2. Pathway enrichment analysis of RNA-Seq data.

Pathway enrichment analysis of RNA-Seq was conducted in BAT obtained from flox/flox and ANKO mice (n=4 per group). Significantly enriched pathways of the up-regulated differentially expressed genes (DEGs, false discovery rate [FDR] < 0.01 and fold change > 2) were identified in the DAVID Bioinformatics Resources (see the Methods section for details).

Supplemental Figure 3

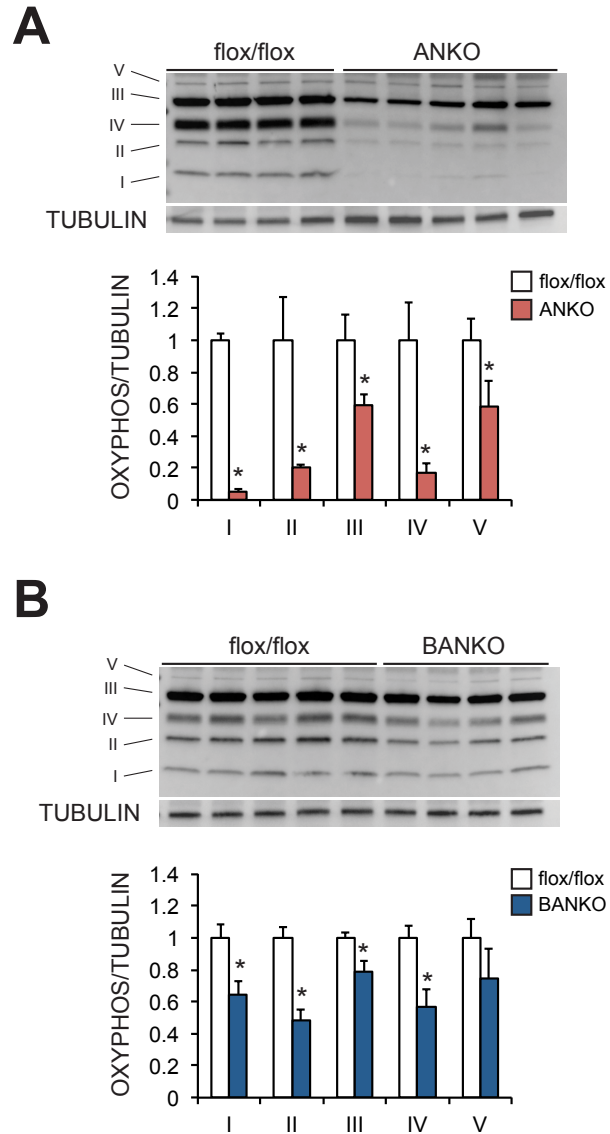


Figure S3. Western blot analysis of subunits of electron transport chain complex in BAT.

Western blot analysis of subunits of electron transport chain complex (I to V) and TUBULIN in BAT obtained from ANKO (A), BANKO (B), and their control (flox/flox) mice ($n=4-5$ per group). Densitometric analysis of each protein normalized to TUBULIN is shown. *Value significantly different from control value (Student's unpaired t-test, $P < 0.05$). Values are means \pm SEM.

Supplemental Figure 4

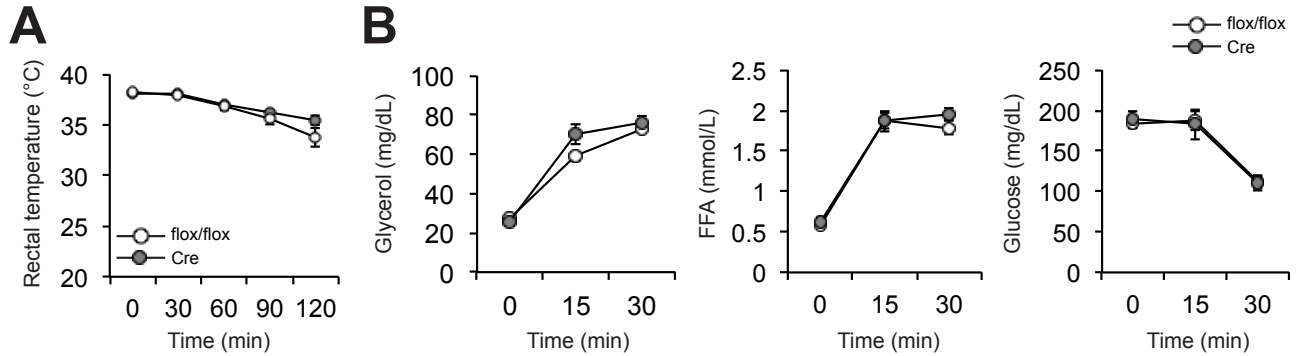


Figure S4. *Adiponectin*-Cre transgenic mice have normal cold tolerance and β 3-adrenergic responses.

(A) Rectal body temperature during cold exposure experiments in *Adiponectin*-Cre transgenic (Cre) and control (flox/flox) mice. Mice were fasted during cold exposure (n=5-6 per group). (B) Plasma concentrations of glycerol and free fatty acids (FFA), and blood glucose concentrations were determined in Cre and flox/flox mice immediately before and 15 and 30 minutes after intraperitoneal injection of CL-316243 (1 mg/kg-body weight) (n=4-7 per group). Values are means \pm SEM.

Supplemental Figure 5

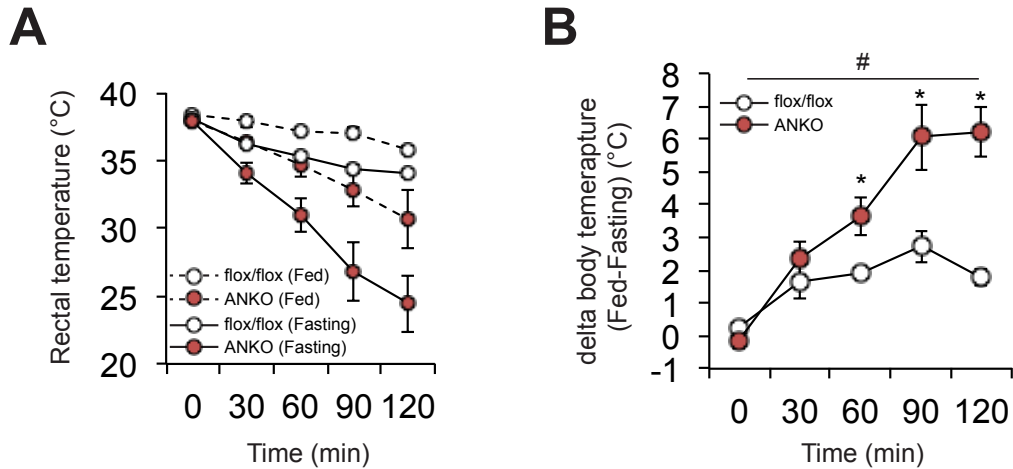


Figure S5. Feeding improves cold tolerance in ANKO mice.

(A) Rectal body temperature during cold exposure experiments in ANKO and control (flox/flox) mice. Mice were fasted or fed during cold exposure (n=5 per group). (B) A body temperature difference (delta) between fasting and fed conditions. #Repeated measures ANOVA revealed a significant group x time interaction (P<0.05). *Value significantly different from control value (Student's unpaired t-test. P<0.05). Values are means \pm SEM.

Supplemental Figure 6

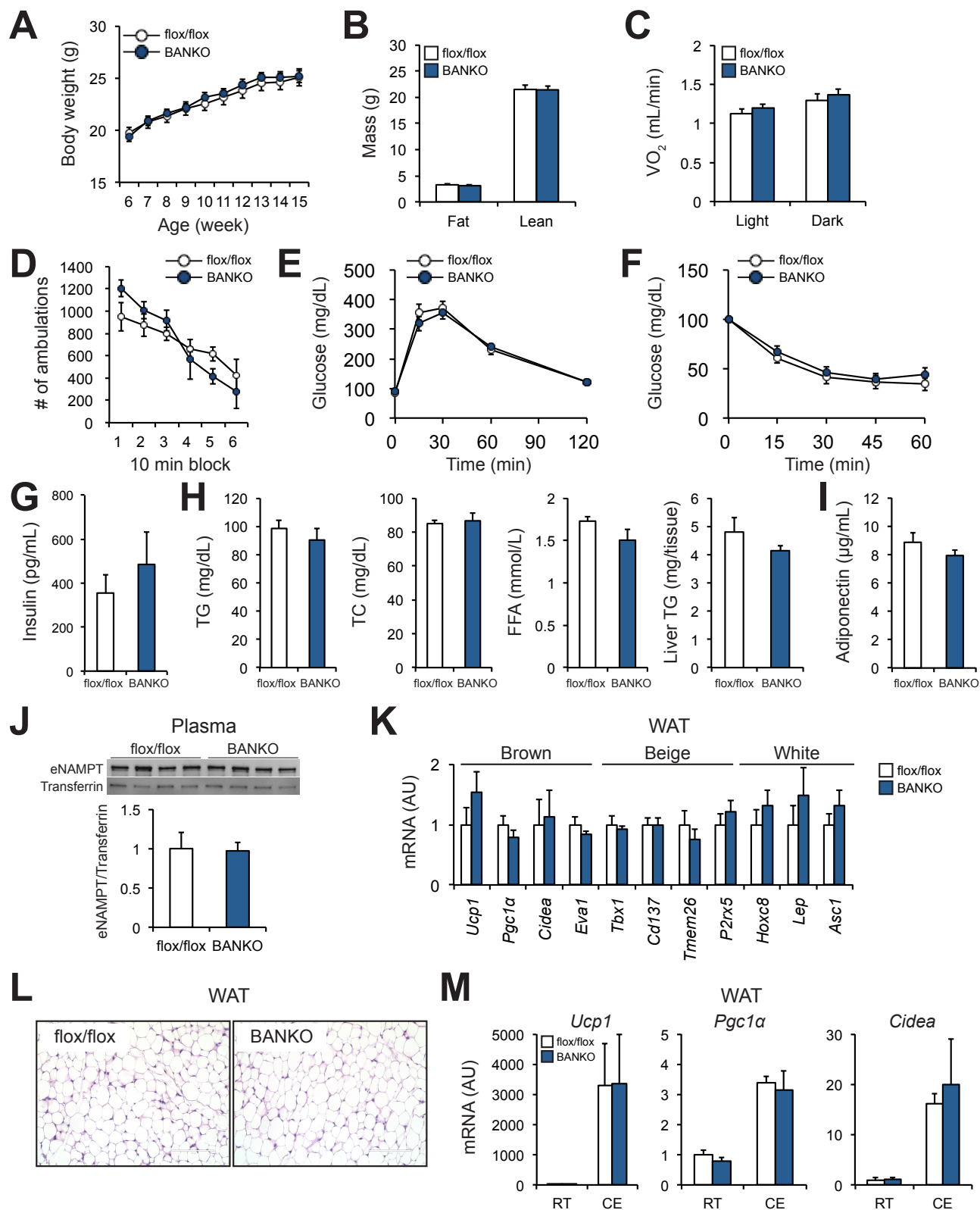


Figure S6. BANKO mice have normal WAT function and glucose metabolism.

Metabolic phenotyping of BANKO and control (flox/flox) mice. (A) Body weight (n=9-10 per group). (B) Body composition (n= 4-5 per group). (C) Whole-body oxygen consumption (mL/hour/mouse, VO_2) values during the 12-hour light and dark periods (n=4 per group). (D) Total ambulations (whole-body movements) during a 1-hour locomotor activity (n=4 per group). Intraperitoneal glucose tolerance tests (IPGTTs) (E) and insulin tolerance tests (ITTs) (F) (n=9-13 per group). (G) Plasma insulin concentrations (n= 9 per group). (H) Plasma concentrations of triglyceride (TG), total cholesterol (TC) and free fatty acids (FFA), and hepatic TG contents (n=5-9 per group). (I) Plasma adiponectin concentrations (n=5 per group). (J) Western blot analysis of plasma extracellular NAMPT (eNAMPT) and transferrin (loading control) (n=4 per group). (K) Inguinal WAT gene expression of brown adipocyte, beige adipocyte, and white adipocyte selective markers, analyzed by real-time PCR (n=4-5 per group). (L) Representative images of haematoxylin and eosin (H&E) staining of inguinal WAT. (M) Inguinal WAT expression of thermogenic genes under room temperature (RT) and following the 24-hour cold exposure (CE) (n=4-5 per group). Values are means \pm SEM.

Supplemental Figure 7

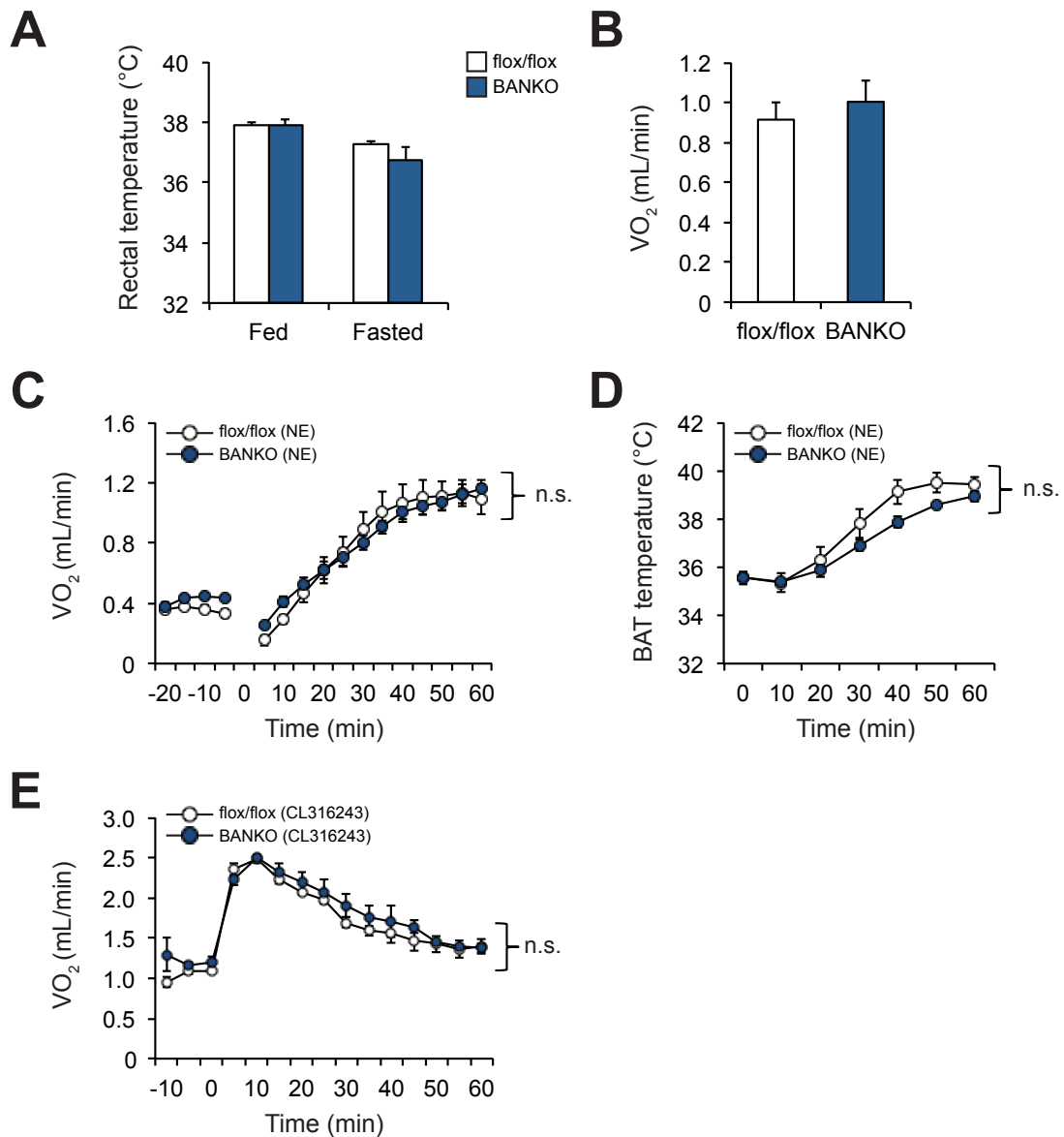


Figure S7. BANKO mice have normal thermogenic and energy responses to fasting and β -adrenergic stimulation.

Thermogenic and energy responses to fasting and β -adrenergic stimulation were determined in BANKO and control (flox/flox) mice. (A) Rectal core body temperature before and after 48 hour fasting (n=7-8 per group). (B) VO_2 during the 12-hour dark period under fasting conditions (n=4 per group). VO_2 values (C) and BAT temperature (D) before and after subcutaneous injection of norepinephrine (NE, 1 mg/kg-body weight) (n=5 per group). (E) VO_2 values before and after intraperitoneal injection of CL-316243 (0.6 mg/kg-body weight) (n=3-4 per group). Values are means \pm SEM.

Supplemental Figure 8

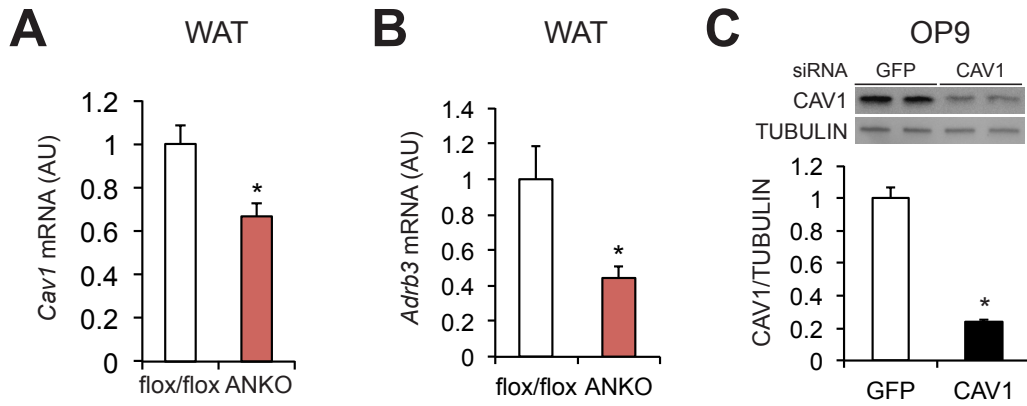


Figure S8. Loss of NAMPT decreases gene expression of Caveolin-1 (*Cav1*) and β 3 adrenergic receptor (*Adrb3*) in WAT.

WAT gene expression of *Cav1* (A) and *Adrb3* (B) in control (flox/flox) and ANKO mice (n=4 per group). (C) Western blot analysis of CAV1 and TUBULIN in GFP or Cav1 siRNA-treated OP9 adipocyte cells (n=4 per group). *Value significantly different from control value (P<0.05). Values are means \pm SEM.

Supplemental Figure 9

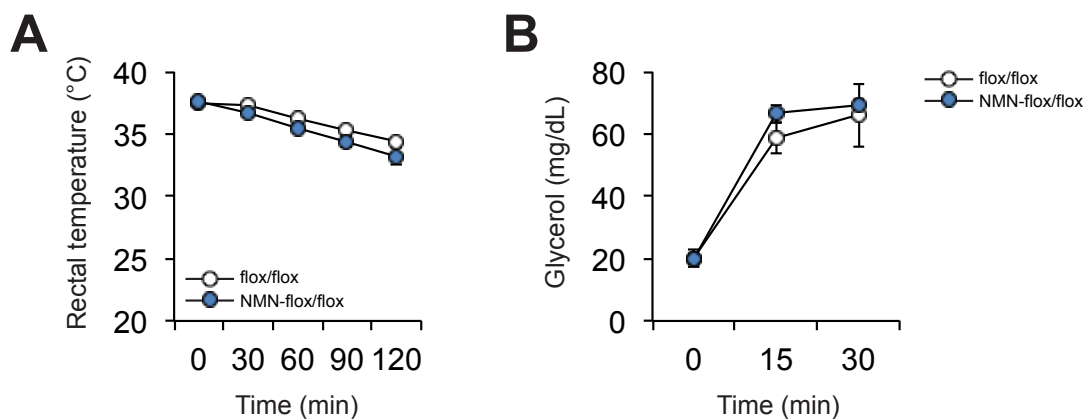


Figure S9. NMN administration has minimal impact on cold tolerance and β 3-adrenergic responses in control (flox/flox) mice.

A key NAD^+ intermediate, NMN, was administered in drinking water to control (flox/flox) mice (1000 mg/kg body weight). Cold tolerance (A) and plasma glycerol concentrations before and after intraperitoneal injection of CL-316243 (1 mg/kg-body weight) (B) were determined in flox/flox and NMN-treated flox/flox mice (n=5 per group). Values are means \pm SEM.

Table S1. Subject characteristics (n=13)

Metabolic parameters	Mean \pm SEM
Age (years)	36.6 \pm 2.6
Body mass index (kg/m ²)	31.0 \pm 0.7
Fat-free mass (kg)	46.6 \pm 1.3
Total body fat (%)	44 \pm 1
Glucose (mg/dL)	87.1 \pm 1.5
Insulin (mU/L)	10.8 \pm 1.3*
Triglyceride (mg/dL)	117.5 \pm 13.2
HDL-cholesterol (mg/dL)	56.5 \pm 3.3
LDL-cholesterol (mg/dL)	95.5 \pm 6.2

Values are means \pm SEM. *n=12.

Abbreviations: HDL, high-density lipoprotein; LDL, low-density lipoprotein.

Table S2. Sequence of primers for real-time PCR

Gene	Accession Number	Primer sequences (5'-3')	
		Forward	Reverse
Mouse			
<i>Nampt</i>	NM_021524	GCAGAAGCCGAGTTCAACATC	TTTTCACGGCATTCAAAGTAGGA
<i>Ucp1</i>	NM_009463	AGGCTTCCAGTACCATTAGGT	CTGAGTGAGGCAAAGCTGATTT
<i>Cyp2b10</i>	NM_009999	AAAGTCCCGTGCAACTTCC	TTGGCTCAACGACAGCAACT
<i>Sgk2</i>	NM_013731	CCATTGGTTACCTTCACTCTCTC	GTCTCCTCAGGCTCTACACAT
<i>Pgc1a</i>	NM_008904	TATGGAGTGACATAGAGTGTGCT	CCACTTCAATCCACCCAGAAAG
<i>Dio2</i>	NM_010050	AATTATGCCTCGGAGAAGACCG	GGCAGTTGCCTAGTGAAAGGT
<i>Ppara</i>	NM_011144	AGAGCCCCATCTGTCTCTC	ACTGGTAGTCTGCAAAACCAA
<i>Lpl</i>	NM_008509	GGGAGTTTGGCTCCAGAGTTT	TGTGTCTTCAGGGGTCCTTAG
<i>Cpt1b</i>	NM_009948	GCACACCAGGCAGTAGCTTT	CAGGAGTTGATTCCAGACAGGTA
<i>Gk</i>	NM_008194	TGGGTAGAACAAGACCCGAAG	GTTGCTGACACCAATGGCTT
<i>Gpam</i>	NM_008149	ACAGTTGGCACAATAGACGTTT	CCTTCCATTTCAAGTGTTCAGA
<i>Acaca</i>	NM_133360	GATGAACCATCTCCGTTGGC	GACCCAATTATGAATCGGGAGTG
<i>Fas</i>	NM_007988	GGAGTGGTGATAGCCGGTAT	TGGTAATCCATAGAGCCCAG
<i>Elovl6</i>	NM_130450	GAAAAGCAGTTCAACGAGAACG	CGGGATTGAATGTTCTTGTCT
<i>Scd1</i>	NM_009127	TTCTTGCGATACACTCTGGTGC	AGATGCCGACCACAAAGATA
<i>Cox1</i>	YP_003024028	GGATTTGTTCACTGATTCCATTA	GCATCTGGGTAGTCTGAGTAGCG
<i>mt-Nd5</i>	NP_904338	CACTCAGACCCAAACATCAATCG	TCGTCCGTACCATCATCCAATTA
<i>Cidea</i>	NM_007702	TGACATTCATGGGATTGCAGAC	GGCCAGTTGTGATGACTAAGAC
<i>Eva1</i>	NM_007962	CCACTTCTCCTGAGTTTACAGC	GCATTTTAACCGAACATCTGTCC
<i>Tbx1</i>	NM_011532	CTGTGGGACGAGTTCAATCAG	TTGTCATCTACGGGCACAAAG
<i>Cd137</i>	NM_011612	CGTGCAGAACTCCTGTGATAAC	GTCACCTATGCTGGAGAAGG
<i>Tmem26</i>	NM_177794	TTCCTGTTGCATTCCCTGGTC	GCCGAGAAAGCCATTTGT
<i>P2rx5</i>	NM_033321	TGGAAGGGGTTTCGTGTTGTC	AGGGAAGTGCAATGTCCTGA
<i>Hoxc8</i>	NM_010466	CTTCGTCAACCCCTGTTTTTC	GTCTTGGACGTGGTGCGAG
<i>Lep</i>	NM_008493	GAGACCCCTGTGTCGGTTC	CTGCGTGTGTGAAATGTCATTG
<i>Asc1</i>	NM_017394	GGGTTTGGCCCTCTTCGTC	GACATAGGCGTAGTCCCCAC
<i>Cav1</i>	NM_001243064	GCGACCCCAAGCATCTCAA	ATGCCGTCGAAACTGTGTGT
<i>Adrb3</i>	NM_013462	GGCCCTCTCTAGTTCCCAG	TAGCCATCAAACCTGTTGAGC
<i>36b4</i>	NM_007475	GCAGACAACGTGGGCTCCAAGCAGAT	GGTCTCTTGGTGAACACGAAGCCC
Human			
<i>NAMPT</i>	NM_005746	AATGTTCTTTCACGGTGGAAAA	ACTGTGATTGGATACCAGGACT
<i>UCP1</i>	NM_021833	AGGTCCAAGGTGAATGCCC	TTACCACAGCGGTGATTGTTC
<i>RPLP0</i>	NM_001002	GTGATGTGCAGCTGATCAAGACT	GATGACCAGCCAAAGGAGA

References

1. Rongvaux A, *et al.* (2008) Nicotinamide phosphoribosyl transferase/pre-B cell colony-enhancing factor/visfatin is required for lymphocyte development and cellular resistance to genotoxic stress. *J Immunol* 181(7):4685-4695.
2. Yoon MJ, *et al.* (2015) SIRT1-Mediated eNAMPT Secretion from Adipose Tissue Regulates Hypothalamic NAD(+) and Function in Mice. *Cell Metab* 21(5):706-717.
3. Stromsdorfer KL, *et al.* (2016) NAMPT-Mediated NAD(+) Biosynthesis in Adipocytes Regulates Adipose Tissue Function and Multi-organ Insulin Sensitivity in Mice. *Cell Rep* 16(7):1851-1860.
4. Chondronikola M, *et al.* (2014) Brown adipose tissue improves whole-body glucose homeostasis and insulin sensitivity in humans. *Diabetes* 63(12):4089-4099.
5. Chondronikola M, *et al.* (2016) Brown Adipose Tissue Activation Is Linked to Distinct Systemic Effects on Lipid Metabolism in Humans. *Cell Metab* 23(6):1200-1206.
6. Chondronikola M, *et al.* (2015) A percutaneous needle biopsy technique for sampling the supraclavicular brown adipose tissue depot of humans. *Int J Obes (Lond)* 39(10):1561-1564.
7. Sidossis L & Kajimura S (2015) Brown and beige fat in humans: thermogenic adipocytes that control energy and glucose homeostasis. *J Clin Invest* 125(2):478-486.
8. Cannon B & Nedergaard J (2004) Brown adipose tissue: function and physiological significance. *Physiol Rev* 84(1):277-359.
9. Kajimura S, Spiegelman BM, & Seale P (2015) Brown and Beige Fat: Physiological Roles beyond Heat Generation. *Cell Metab* 22(4):546-559.
10. Porter LC, *et al.* (2018) NAD(+)-dependent deacetylase SIRT3 in adipocytes is dispensable for maintaining normal adipose tissue mitochondrial function and whole body metabolism. *Am J Physiol Endocrinol Metab* 315(4):E520-E530.
11. Sasaki Y, Hackett AR, Kim S, Strickland A, & Milbrandt J (2018) Dysregulation of NAD(+) Metabolism Induces a Schwann Cell Dedifferentiation Program. *J Neurosci* 38(29):6546-6562.
12. Yoshino J & Imai S (2013) Accurate measurement of nicotinamide adenine dinucleotide (NAD(+)) with high-performance liquid chromatography. *Methods Mol Biol* 1077:203-215.